

Measurement of the absolute branching fraction for $\Lambda_c^+ \rightarrow \Lambda \mu^+ \nu_\mu$ 

BESIII Collaboration

M. Ablikim^a, M.N. Achasov^{i,5}, S. Ahmedⁿ, X.C. Ai^a, O. Albayrak^e, M. Albrecht^d, D.J. Ambrose^{aw}, A. Amoroso^{bb, bd}, F.F. An^a, Q. An^{ay, 1}, J.Z. Bai^a, O. Bakina^y, R. Baldini Ferroli^t, Y. Ban^{ag}, D.W. Bennett^s, J.V. Bennett^e, N. Berger^x, M. Bertani^t, D. Bettoni^v, J.M. Bian^{av}, F. Bianchi^{bb, bd}, E. Boger^{y, 3}, I. Boyko^y, R.A. Briere^e, H. Cai^{bf}, X. Cai^{a, 1}, O. Cakir^{ap}, A. Calcaterra^t, G.F. Cao^a, S.A. Cetin^{aq}, J.F. Chang^{a, 1}, G. Chelkov^{y, 3, 4}, G. Chen^a, H.S. Chen^a, J.C. Chen^a, M.L. Chen^{a, 1}, S. Chen^{at}, S.J. Chen^{ae}, X. Chen^{a, 1}, X.R. Chen^{ab}, Y.B. Chen^{a, 1}, X.K. Chu^{ag}, G. Cibinetto^v, H.L. Dai^{a, 1}, J.P. Dai^{aj}, A. Dbeyssiⁿ, D. Dedovich^y, Z.Y. Deng^a, A. Denig^x, I. Denysenko^y, M. Destefanis^{bb, bd}, F. De Mori^{bb, bd}, Y. Ding^{ac}, C. Dong^{af}, J. Dong^{a, 1}, L.Y. Dong^a, M.Y. Dong^{a, 1}, Z.L. Dou^{ae}, S.X. Du^{bh}, P.F. Duan^a, J.Z. Fan^{ao}, J. Fang^{a, 1}, S.S. Fang^a, X. Fang^{ay, 1}, Y. Fang^a, R. Farinelli^{v, w}, L. Fava^{bc, bd}, F. Feldbauer^x, G. Felici^t, C.Q. Feng^{ay, 1}, E. Fioravanti^v, M. Fritsch^{n, x}, C.D. Fu^a, Q. Gao^a, X.L. Gao^{ay, 1}, Y. Gao^{ao}, Z. Gao^{ay, 1}, I. Garzia^v, K. Goetzen^j, L. Gong^{af}, W.X. Gong^{a, 1}, W. Gradl^x, M. Greco^{bb, bd}, M.H. Gu^{a, 1}, Y.T. Gu^l, Y.H. Guan^a, A.Q. Guo^a, L.B. Guo^{ad}, R.P. Guo^a, Y. Guo^a, Y.P. Guo^x, Z. Haddadi^{aa}, A. Hafner^x, S. Han^{bf}, X.Q. Hao^o, F.A. Harris^{au}, K.L. He^a, F.H. Heinsius^d, T. Held^d, Y.K. Heng^{a, 1}, T. Holtmann^d, Z.L. Hou^a, C. Hu^{ad}, H.M. Hu^a, J.F. Hu^{bb, bd}, T. Hu^{a, 1}, Y. Hu^a, G.S. Huang^{ay, 1}, J.S. Huang^o, X.T. Huang^{ai}, X.Z. Huang^{ae}, Z.L. Huang^{ac}, T. Hussain^{ba}, W. Ikegami Andersson^{be}, Q. Ji^a, Q.P. Ji^o, X.B. Ji^a, X.L. Ji^{a, 1}, L.W. Jiang^{bf}, X.S. Jiang^{a, 1}, X.Y. Jiang^{af}, J.B. Jiao^{ai}, Z. Jiao^q, D.P. Jin^{a, 1}, S. Jin^a, T. Johansson^{be}, A. Julin^{av}, N. Kalantar-Nayestanaki^{aa}, X.L. Kang^a, X.S. Kang^{af}, M. Kavatsyuk^{aa}, B.C. Ke^e, P. Kiese^x, R. Kliemt^j, B. Kloss^x, O.B. Kolcu^{aq, 8}, B. Kopf^d, M. Kornicer^{au}, A. Kupsc^{be}, W. Kühn^z, J.S. Lange^z, M. Lara^s, P. Larinⁿ, L. Lavezzi^{bd, a}, H. Leithoff^x, C. Leng^{bd}, C. Li^{be}, Li Cheng^{ay, 1}, D.M. Li^{bh}, F. Li^{a, 1}, F.Y. Li^{ag}, G. Li^a, H.B. Li^a, H.J. Li^a, J.C. Li^a, Jin Li^{ah}, K. Li^m, K. Li^{ai}, Lei. Li^{c, *}, P.R. Li^{g, at}, Q.Y. Li^{ai}, T. Li^{ai}, W.D. Li^a, W.G. Li^a, X.L. Li^{ai}, X.N. Li^{a, 1}, X.Q. Li^{af}, Y.B. Li^b, Z.B. Li^{an}, H. Liang^{ay, 1}, Y.F. Liang^{al}, Y.T. Liang^z, G.R. Liao^k, D.X. Linⁿ, B. Liu^{aj}, B.J. Liu^a, C.X. Liu^a, D. Liu^{ay, 1}, F.H. Liu^{ak}, Fang Liu^a, Feng Liu^f, H.B. Liu^l, H.H. Liu^a, H.H. Liu^p, H.M. Liu^a, J. Liu^a, J.B. Liu^{ay, 1}, J.P. Liu^{bf}, J.Y. Liu^a, K. Liu^{ao}, K.Y. Liu^{ac}, L.D. Liu^{ag}, P.L. Liu^{a, 1}, Q. Liu^{at}, Q.J. Liu^c, S.B. Liu^{ay, 1}, X. Liu^{ab}, Y.B. Liu^{af}, Y.Y. Liu^{af}, Z.A. Liu^{a, 1}, Z.Q. Liu^x, H. Loehner^{aa}, X.C. Lou^{a, 1, 7}, H.J. Lu^q, J.G. Lu^{a, 1}, Y. Lu^a, Y.P. Lu^{a, 1}, C.L. Luo^{ad}, M.X. Luo^{bg}, T. Luo^{au}, X.L. Luo^{a, 1}, X.R. Lyu^{at}, F.C. Ma^{ac}, H.L. Ma^a, L.L. Ma^{ai}, M.M. Ma^a, Q.M. Ma^a, T. Ma^a, X.N. Ma^{af}, X.Y. Ma^{a, 1}, Y.M. Ma^{ai}, F.E. Maasⁿ, M. Maggiora^{bb, bd}, Q.A. Malik^{ba}, Y.J. Mao^{ag}, Z.P. Mao^a, S. Marcello^{bb, bd}, J.G. Messchendorp^{aa}, G. Mezzadri^w, J. Min^{a, 1}, T.J. Min^a, R.E. Mitchell^s, X.H. Mo^{a, 1}, Y.J. Mo^f, C. Morales Moralesⁿ, N.Yu. Muchnoi^{i, 5}, H. Muramatsu^{av}, P. Musiol^d, Y. Nefedov^y, F. Nerling^j, I.B. Nikolaev^{i, 5}, Z. Ning^{a, 1}, S. Nisar^h, S.L. Niu^{a, 1}, X.Y. Niu^a, S.L. Olsen^{ah}, Q. Ouyang^{a, 1}, S. Pacetti^u, Y. Pan^{ay, 1}, P. Patteri^t, M. Pelizaeus^d, H.P. Peng^{ay, 1}, K. Peters^{j, 9}, J. Pettersson^{be}, J.L. Ping^{ad}, R.G. Ping^a, R. Poling^{av}, V. Prasad^a, H.R. Qi^b, M. Qi^{ae}, S. Qian^{a, 1}, C.F. Qiao^{at}, L.Q. Qin^{ai}, N. Qin^{bf}, X.S. Qin^a, Z.H. Qin^{a, 1}, J.F. Qiu^a

K.H. Rashid^{ba}, C.F. Redmer^x, M. Ripka^x, G. Rong^a, Ch. Rosnerⁿ, X.D. Ruan^l,
 A. Sarantsev^{y,6}, M. Savrié^w, C. Schnier^d, K. Schoenning^{be}, W. Shan^{ag}, M. Shao^{ay,1},
 C.P. Shen^b, P.X. Shen^{af}, X.Y. Shen^a, H.Y. Sheng^a, W.M. Song^a, X.Y. Song^a, S. Sosio^{bb,bd},
 S. Spataro^{bb,bd}, G.X. Sun^a, J.F. Sun^o, S.S. Sun^a, X.H. Sun^a, Y.J. Sun^{ay,1}, Y.Z. Sun^a,
 Z.J. Sun^{a,1}, Z.T. Sun^s, C.J. Tang^{al}, X. Tang^a, I. Tapan^{ar}, E.H. Thorndike^{aw}, M. Tiemens^{aa},
 I. Uman^{as}, G.S. Varner^{au}, B. Wang^{af}, B.L. Wang^{at}, D. Wang^{ag}, D.Y. Wang^{ag}, K. Wang^{a,1},
 L.L. Wang^a, L.S. Wang^a, M. Wang^{ai}, P. Wang^a, P.L. Wang^a, W. Wang^{a,1}, W.P. Wang^{ay,1},
 X.F. Wang^{ao}, Y. Wang^{am}, Y.D. Wangⁿ, Y.F. Wang^{a,1}, Y.Q. Wang^x, Z. Wang^{a,1}, Z.G. Wang^{a,1},
 Z.H. Wang^{ay,1}, Z.Y. Wang^a, T. Weber^x, D.H. Wei^k, P. Weidenkaff^x, S.P. Wen^a,
 U. Wiedner^d, M. Wolke^{be}, L.H. Wu^a, L.J. Wu^a, Z. Wu^{a,1}, L. Xia^{ay,1}, L.G. Xia^{ao}, Y. Xia^r,
 D. Xiao^a, H. Xiao^{az}, Z.J. Xiao^{ad}, Y.G. Xie^{a,1}, Xie Yuehong^f, Q.L. Xiu^{a,1}, G.F. Xu^a, J.J. Xu^a,
 L. Xu^a, Q.J. Xu^m, Q.N. Xu^{at}, X.P. Xu^{am}, L. Yan^{bb,bd}, W.B. Yan^{ay,1}, W.C. Yan^{ay,1}, Y.H. Yan^r,
 H.J. Yang^{aj,10}, H.X. Yang^a, L. Yang^{bf}, Y.X. Yang^k, M. Ye^{a,1}, M.H. Ye^g, J.H. Yin^a, Z.Y. You^{an},
 B.X. Yu^{a,1}, C.X. Yu^{af}, J.S. Yu^{ab}, C.Z. Yuan^a, Y. Yuan^a, A. Yuncu^{aq,2}, A.A. Zafar^{ba}, Y. Zeng^r,
 Z. Zeng^{ay,1}, B.X. Zhang^a, B.Y. Zhang^{a,1}, C.C. Zhang^a, D.H. Zhang^a, H.H. Zhang^{an},
 H.Y. Zhang^{a,1}, J. Zhang^a, J.J. Zhang^a, J.L. Zhang^a, J.Q. Zhang^a, J.W. Zhang^{a,1}, J.Y. Zhang^a,
 J.Z. Zhang^a, K. Zhang^a, L. Zhang^a, S.Q. Zhang^{af}, X.Y. Zhang^{ai}, Y. Zhang^a, Y.H. Zhang^{a,1},
 Y.N. Zhang^{at}, Y.T. Zhang^{ay,1}, Yu Zhang^{at}, Z.H. Zhang^f, Z.P. Zhang^{ay}, Z.Y. Zhang^{bf}, G. Zhao^a,
 J.W. Zhao^{a,1}, J.Y. Zhao^a, J.Z. Zhao^{a,1}, Lei Zhao^{ay,1}, Ling Zhao^a, M.G. Zhao^{af}, Q. Zhao^a,
 Q.W. Zhao^a, S.J. Zhao^{bh}, T.C. Zhao^a, Y.B. Zhao^{a,1}, Z.G. Zhao^{ay,1}, A. Zhemchugov^{y,3},
 B. Zheng^{az}, J.P. Zheng^{a,1}, W.J. Zheng^{ai}, Y.H. Zheng^{at}, B. Zhong^{ad}, L. Zhou^{a,1}, X. Zhou^{bf},
 X.K. Zhou^{ay,1}, X.R. Zhou^{ay,1}, X.Y. Zhou^a, K. Zhu^a, K.J. Zhu^{a,1}, S. Zhu^a, S.H. Zhu^{ax},
 X.L. Zhu^{ao}, Y.C. Zhu^{ay,1}, Y.S. Zhu^a, Z.A. Zhu^a, J. Zhuang^{a,1}, L. Zotti^{bb,bd}, B.S. Zou^a,
 J.H. Zou^a

^a Institute of High Energy Physics, Beijing 100049, People's Republic of China^b Beihang University, Beijing 100191, People's Republic of China^c Beijing Institute of Petrochemical Technology, Beijing 102617, People's Republic of China^d Bochum Ruhr-University, D-44780 Bochum, Germany^e Carnegie Mellon University, Pittsburgh, PA 15213, USA^f Central China Normal University, Wuhan 430079, People's Republic of China^g China Center of Advanced Science and Technology, Beijing 100190, People's Republic of China^h COMSATS Institute of Information Technology, Lahore, Defence Road, Off Raiwind Road, 54000 Lahore, Pakistanⁱ G.I. Budker Institute of Nuclear Physics SB RAS (BINP), Novosibirsk 630090, Russia^j GSI Helmholtzcentre for Heavy Ion Research GmbH, D-64291 Darmstadt, Germany^k Guangxi Normal University, Guilin 541004, People's Republic of China^l Guangxi University, Nanning 530004, People's Republic of China^m Hangzhou Normal University, Hangzhou 310036, People's Republic of Chinaⁿ Helmholtz Institute Mainz, Johann-Joachim-Becher-Weg 45, D-55099 Mainz, Germany^o Henan Normal University, Xinxiang 453007, People's Republic of China^p Henan University of Science and Technology, Luoyang 471003, People's Republic of China^q Huangshan College, Huangshan 245000, People's Republic of China^r Hunan University, Changsha 410082, People's Republic of China^s Indiana University, Bloomington, IN 47405, USA^t INFN Laboratori Nazionali di Frascati, I-00044, Frascati, Italy^u INFN and University of Perugia, I-06100, Perugia, Italy^v INFN Sezione di Ferrara, I-44122, Ferrara, Italy^w University of Ferrara, I-44122, Ferrara, Italy^x Johannes Gutenberg University of Mainz, Johann-Joachim-Becher-Weg 45, D-55099 Mainz, Germany^y Joint Institute for Nuclear Research, 141980 Dubna, Moscow region, Russia^z Justus-Liebig-Universität Giessen, II. Physikalisches Institut, Heinrich-Buff-Ring 16, D-35392 Giessen, Germany^{aa} KVI-CART, University of Groningen, NL-9747 AA Groningen, The Netherlands^{ab} Lanzhou University, Lanzhou 730000, People's Republic of China^{ac} Liaoning University, Shenyang 110036, People's Republic of China^{ad} Nanjing Normal University, Nanjing 210023, People's Republic of China^{ae} Nanjing University, Nanjing 210093, People's Republic of China^{af} Nankai University, Tianjin 300071, People's Republic of China^{ag} Peking University, Beijing 100871, People's Republic of China^{ah} Seoul National University, Seoul, 151-747, Republic of Korea^{ai} Shandong University, Jinan 250100, People's Republic of China^{aj} Shanghai Jiao Tong University, Shanghai 200240, People's Republic of China^{ak} Shanxi University, Taiyuan 030006, People's Republic of China^{al} Sichuan University, Chengdu 610064, People's Republic of China^{am} Soochow University, Suzhou 215006, People's Republic of China^{an} Sun Yat-Sen University, Guangzhou 510275, People's Republic of China^{ao} Tsinghua University, Beijing 100084, People's Republic of China^{ap} Ankara University, 06100 Tandogan, Ankara, Turkey

- ^{aq} Istanbul Bilgi University, 34060 Eyup, Istanbul, Turkey
^{ar} Uludag University, 16059 Bursa, Turkey
^{as} Near East University, Nicosia, North Cyprus, Mersin 10, Turkey
^{at} University of Chinese Academy of Sciences, Beijing 100049, People's Republic of China
^{au} University of Hawaii, Honolulu, HI 96822, USA
^{av} University of Minnesota, Minneapolis, MN 55455, USA
^{aw} University of Rochester, Rochester, NY 14627, USA
^{ax} University of Science and Technology, Liaoning, Anshan 114051, People's Republic of China
^{ay} University of Science and Technology of China, Hefei 230026, People's Republic of China
^{az} University of South China, Hengyang 421001, People's Republic of China
^{ba} University of the Punjab, Lahore 54590, Pakistan
^{bb} University of Turin, I-10125, Turin, Italy
^{bc} University of Eastern Piedmont, I-15121, Alessandria, Italy
^{bd} INFN, I-10125, Turin, Italy
^{be} Uppsala University, Box 516, SE-75120 Uppsala, Sweden
^{bf} Wuhan University, Wuhan 430072, People's Republic of China
^{bg} Zhejiang University, Hangzhou 310027, People's Republic of China
^{bh} Zhengzhou University, Zhengzhou 450001, People's Republic of China

ARTICLE INFO

Article history:

Received 14 November 2016
 Received in revised form 18 January 2017
 Accepted 21 January 2017
 Available online 27 January 2017
 Editor: W.-D. Schlatter

Keywords:

Λ_c^+
 Semi-leptonic decay
 Absolute branching fraction
 BESIII

ABSTRACT

We report the first measurement of the absolute branching fraction for $\Lambda_c^+ \rightarrow \Lambda\mu^+\nu_\mu$. This measurement is based on a sample of e^+e^- annihilation data produced at a center-of-mass energy $\sqrt{s} = 4.6$ GeV, collected with the BESIII detector at the BEPCII storage rings. The sample corresponds to an integrated luminosity of 567 pb^{-1} . The branching fraction is determined to be $\mathcal{B}(\Lambda_c^+ \rightarrow \Lambda\mu^+\nu_\mu) = (3.49 \pm 0.46(\text{stat}) \pm 0.27(\text{syst}))\%$. In addition, we calculate the ratio $\mathcal{B}(\Lambda_c^+ \rightarrow \Lambda\mu^+\nu_\mu)/\mathcal{B}(\Lambda_c^+ \rightarrow \Lambda e^+\nu_e)$ to be $0.96 \pm 0.16(\text{stat}) \pm 0.04(\text{syst})$.

© 2017 The Author(s). Published by Elsevier B.V. This is an open access article under the CC BY license (<http://creativecommons.org/licenses/by/4.0/>). Funded by SCOAP³.

1. Introduction

Semileptonic (SL) decays of the lightest charmed baryon, Λ_c^+ , provide a stringent test for non-perturbative aspects of the strong interaction theory. The $\Lambda_c^+ \rightarrow \Lambda\ell^+\nu_\ell$ (ℓ denotes lepton) decay is dominated by the Cabibbo-favored transition $c \rightarrow s\ell^+\nu_\ell$, which occurs independently of the spin-zero and isospin-zero spectator ud diquark, to good approximation. This leads to a simpler theoretical description and greater predictive power in the non-perturbative models than in the case for charmed mesons [1]. Predictions of the branching fraction (BF) $\mathcal{B}(\Lambda_c^+ \rightarrow \Lambda\ell^+\nu_\ell)$ in different theoretical models vary over a wide range from 1.4% to 9.2% [2–13], depending on the choice of Λ_c^+ wave function model and the treatment of decay dynamics. In 2015, BESIII measured the absolute BF for $\Lambda_c^+ \rightarrow \Lambda e^+\nu_e$ to be $\mathcal{B}(\Lambda_c^+ \rightarrow \Lambda e^+\nu_e) = (3.63 \pm 0.38 \pm 0.20)\%$ [14], which disfavors the predictions in Refs. [2,3,5–7] at 95% confidence level. It is desirable to confirm the result of $\mathcal{B}(\Lambda_c^+ \rightarrow \Lambda e^+\nu_e)$ by measuring the corresponding muonic SL decay BF $\mathcal{B}(\Lambda_c^+ \rightarrow \Lambda\mu^+\nu_\mu)$,

which provides further test on these theoretical predictions with more experimental data. In addition, lepton universality can be tested by comparing the BFs between the electronic and muonic decay modes.

In this paper, we report the first absolute measurement of $\mathcal{B}(\Lambda_c^+ \rightarrow \Lambda\mu^+\nu_\mu)$ by analyzing a data sample corresponding to an integrated luminosity of 567 pb^{-1} [15] collected at a center-of-mass (c.m.) energy of $\sqrt{s} = 4.6$ GeV by the BESIII detector at the BEPCII collider. This is the largest e^+e^- collision data sample near the $\Lambda_c^+\bar{\Lambda}_c^-$ mass threshold. At this energy, the Λ_c^+ is produced in association with one $\bar{\Lambda}_c^-$ baryon only, and no other hadrons are kinematically allowed. Hence, $\mathcal{B}(\Lambda_c^+ \rightarrow \Lambda\mu^+\nu_\mu)$ can be accessed by measuring the relative probability of finding the SL decay when the $\bar{\Lambda}_c^-$ is detected in a number of prolific decay channels. This will provide a straightforward and direct BF measurement without requiring knowledge of the total number of $\Lambda_c^+\bar{\Lambda}_c^-$ pairs produced. In the following, charge conjugated modes are always implied, unless explicitly mentioned.

2. BESIII detector and Monte Carlo simulation

The BESIII [16] detector is a cylindrical detector with a solid-angle coverage of 93% of 4π that operates at the BEPCII collider. It consists of a Helium-gas based main drift chamber (MDC), a plastic scintillator time-of-flight (TOF) system, a CsI (TI) electromagnetic calorimeter (EMC), a superconducting solenoid providing a 1.0 T magnetic field and a muon counter. The charged particle momentum resolution is 0.5% at a transverse momentum of 1 GeV/c. The photon energy resolution in the EMC is 2.5% in the barrel and 5.0% in the end-caps at 1 GeV. More details about the design and performance of the detector are given in Ref. [16].

A GEANT4-based [17] Monte Carlo (MC) simulation package, which includes the geometric description of the detector and the

* Corresponding author.

E-mail address: lilei2014@bipt.edu.cn (Lei. Li).

¹ Also at State Key Laboratory of Particle Detection and Electronics, Beijing 100049, Hefei 230026, People's Republic of China.

² Also at Bogazici University, 34342 Istanbul, Turkey.

³ Also at the Moscow Institute of Physics and Technology, Moscow 141700, Russia.

⁴ Also at the Functional Electronics Laboratory, Tomsk State University, Tomsk 634050, Russia.

⁵ Also at the Novosibirsk State University, Novosibirsk 630090, Russia.

⁶ Also at the NRC “Kurchatov Institute”, PNPI, 188300, Gatchina, Russia.

⁷ Also at University of Texas at Dallas, Richardson, TX 75083, USA.

⁸ Also at Istanbul Arel University, 34295 Istanbul, Turkey.

⁹ Also at Goethe University Frankfurt, 60323 Frankfurt am Main, Germany.

¹⁰ Also at Institute of Nuclear and Particle Physics, Shanghai Key Laboratory for Particle Physics and Cosmology, Shanghai 200240, People's Republic of China.

Table 1
ST decay modes, ΔE requirements and yields ($N_{\bar{\Lambda}_c^-}$) in data. Yields uncertainties are statistical only.

Mode	ΔE (GeV)	$N_{\bar{\Lambda}_c^-}$
$\bar{p}K_S^0$	[-0.025, 0.028]	1066 ± 33
$\bar{p}K^+\pi^-$	[-0.019, 0.023]	5692 ± 88
$\bar{p}K_S^0\pi^0$	[-0.035, 0.049]	593 ± 41
$\bar{p}K^+\pi^-\pi^0$	[-0.044, 0.052]	1547 ± 61
$\bar{p}K_S^0\pi^+\pi^-$	[-0.029, 0.032]	516 ± 34
$\bar{\Lambda}\pi^-$	[-0.033, 0.035]	593 ± 25
$\bar{\Lambda}\pi^-\pi^0$	[-0.037, 0.052]	1864 ± 56
$\bar{\Lambda}\pi^-\pi^+\pi^-$	[-0.028, 0.030]	674 ± 36
$\bar{\Sigma}^0\pi^-$	[-0.029, 0.032]	532 ± 30
$\bar{\Sigma}^-\pi^0$	[-0.038, 0.062]	329 ± 28
$\bar{\Sigma}^-\pi^+\pi^-$	[-0.049, 0.054]	1009 ± 57

detector response, is used to determine the detection efficiency and to estimate the potential backgrounds. Signal MC samples of a Λ_c^+ baryon decaying only to $\Lambda\mu^+\nu_\mu$ together with a $\bar{\Lambda}_c^-$ decaying to specified modes are generated with the KKMC [18] event generator using EVTGEN [19], taking into account the initial state radiation (ISR) [20] and the final state radiation (FSR) [21] effects. For the simulation of the process $\Lambda_c^+ \rightarrow \Lambda\mu^+\nu_\mu$, we use the form factor obtained using Heavy Quark Effective Theory and QCD sum rules of Ref. [10]. To study backgrounds, inclusive MC samples are simulated, which consist of $\Lambda_c^+\bar{\Lambda}_c^-$ events, $D_{(s)}^{(*)}\bar{D}_{(s)}^{(*)} + X$ production (i.e., all the allowed charmed meson production channels in the c.m. energy), ISR return to the charmonium(-like) ψ states at lower masses, and QED processes. The decay modes with measured BF of the Λ_c , ψ and $D_{(s)}^{(*)}$ particles, are simulated with EVTGEN, using as input the BF of the Particle Data Group (PDG) [22] while the remaining unmeasured decays are generated with LUNDCHARM [23].

3. Analysis

Following the similar technique of the single tag (ST) and double tag (DT) in Ref. [14], we select a data sample (the ST sample) where a $\bar{\Lambda}_c^-$ baryon candidate is reconstructed in one of the eleven exclusive hadronic decay modes listed in the first column of Table 1, then we search in this sample for $\Lambda_c^+ \rightarrow \Lambda\mu^+\nu_\mu$ candidates, which are reconstructed using the remaining tracks recoiling against the ST $\bar{\Lambda}_c^-$ candidate. The events where a pair of $\Lambda_c^+\bar{\Lambda}_c^-$ is reconstructed are the DT sample.

In the ST sample, the intermediate particles of the K_S^0 , $\bar{\Lambda}$, $\bar{\Sigma}^0$, $\bar{\Sigma}^-$ and π^0 are reconstructed through their decays $K_S^0 \rightarrow \pi^+\pi^-$, $\bar{\Lambda} \rightarrow \bar{p}\pi^+$, $\bar{\Sigma}^0 \rightarrow \gamma\bar{\Lambda}$ with $\bar{\Lambda} \rightarrow \bar{p}\pi^+$, $\bar{\Sigma}^- \rightarrow \bar{p}\pi^0$ and $\pi^0 \rightarrow \gamma\gamma$, respectively. The detailed selection criteria for charged and neutral tracks, π^0 , K_S^0 and $\bar{\Lambda}$ candidates used in the reconstruction of tags are described in Ref. [14]. The ST $\bar{\Lambda}_c^-$ signals are identified using the beam energy constrained mass, $M_{BC} = \sqrt{E_{\text{beam}}^2/c^4 - |\vec{p}_{\bar{\Lambda}_c^-}|^2/c^2}$, where E_{beam} is the beam energy and $\vec{p}_{\bar{\Lambda}_c^-}$ is the momentum of the $\bar{\Lambda}_c^-$ candidate. To improve the signal purity, the energy difference $\Delta E = E_{\text{beam}} - E_{\bar{\Lambda}_c^-}$ for each candidate is required to be within $\pm 3\sigma_{\Delta E}$ around the ΔE peak, where $\sigma_{\Delta E}$ is the ΔE resolution and $E_{\bar{\Lambda}_c^-}$ is the reconstructed $\bar{\Lambda}_c^-$ energy. Table 1 shows the mode dependent ΔE requirements and the ST yields in the M_{BC} signal region (2.280, 2.296) GeV/ c^2 , which are obtained by a fit to the M_{BC} distributions. The detailed process to extract the ST signal yields is described in Ref. [14]. The total ST yield summed over all 11 modes is $N_{\bar{\Lambda}_c^-}^{\text{tot}} = 14415 \pm 159$, where the uncertainty is statistical only.

The Λ candidate from the $\bar{\Lambda}_c^-$ decays is formed from a $p\pi^-$ combination that is constrained by a common vertex fit to have a positive decay length L [14]. If multiple Λ candidates are formed,

the one with the largest L/σ_L is retained, where σ_L is the resolution of the measured L . Particle identification (PID) is performed using probabilities derived combining the measurements of the specific energy loss dE/dx by the MDC, the time of flight by the TOF, and of the energy by the EMC; a μ candidate is required to satisfy $\mathcal{L}'_\mu > 0.001$, $\mathcal{L}'_\mu > \mathcal{L}'_e$ and $\mathcal{L}'_\mu > \mathcal{L}'_K$, where \mathcal{L}'_μ , \mathcal{L}'_e , and \mathcal{L}'_K are the probabilities for a muon, electron, and kaon, respectively.

Studies on the inclusive MC samples show that the backgrounds are dominated by $\Lambda_c^+ \rightarrow \Lambda\pi^+$, $\Sigma^0\pi^+$ and $\Lambda\pi^+\pi^0$. Backgrounds from $\Lambda_c^+ \rightarrow \Lambda\pi^+$ and $\Lambda_c^+ \rightarrow \Sigma^0\pi^+$ are rejected by requiring the $\Lambda\mu^+$ invariant mass, $M_{\Lambda\mu^+}$, less than 2.12 GeV/ c^2 . The background from $\Lambda_c^+ \rightarrow \Lambda\pi^+\pi^0$ is suppressed by requiring the largest energy of any unused photons $E_{\gamma\text{max}}$ be less than 0.25 GeV and the deposited energy for the muon candidate in the EMC be less than 0.30 GeV.

Since the neutrino is not detected, we employ the kinematic variable $U_{\text{miss}} \equiv E_{\text{miss}} - c|\vec{p}_{\text{miss}}|$ to identify the neutrino signal, where E_{miss} and \vec{p}_{miss} are the missing energy and momentum carried by the neutrino, respectively. They are calculated as $E_{\text{miss}} = E_{\text{beam}} - E_\Lambda - E_{\mu^+}$ and $\vec{p}_{\text{miss}} = \vec{p}_{\Lambda_c^+} - \vec{p}_\Lambda - \vec{p}_{\mu^+}$, where $\vec{p}_{\Lambda_c^+}$ is the momentum of the Λ_c^+ baryon, E_Λ (\vec{p}_Λ) and E_{μ^+} (\vec{p}_{μ^+}) are the energies (momenta) of the Λ and μ^+ , respectively. Here, the momentum $\vec{p}_{\Lambda_c^+}$ is given by $\vec{p}_{\Lambda_c^+} = -\hat{p}_{\text{tag}}\sqrt{E_{\text{beam}}^2/c^2 - m_{\bar{\Lambda}_c^-}^2}$, where \hat{p}_{tag} is the momentum direction of the ST $\bar{\Lambda}_c^-$ and $m_{\bar{\Lambda}_c^-}$ is the nominal $\bar{\Lambda}_c^-$ mass [22]. For the signal events, the U_{miss} distribution is expected to peak at zero.

The distribution of the $p\pi^-$ invariant mass $M_{p\pi^-}$ versus U_{miss} for the $\Lambda_c^+ \rightarrow \Lambda\mu^+\nu_\mu$ candidates in data is shown in Fig. 1 (a), where a cluster around the signal region is evident. After requiring $M_{p\pi^-}$ to be within the Λ signal region (1.110, 1.121) GeV/ c^2 [14], the projection of U_{miss} is shown in Fig. 1(b). Two bumps, which correspond to the signal peak (left side) and background $\Lambda_c^+ \rightarrow \Lambda\pi^+\pi^0$ (right side), are visible. According to MC simulations, the survival rate of the background process $\Lambda_c^+ \rightarrow \Lambda\pi^+\pi^0$ is estimated to be $\eta_{\Lambda\pi^+\pi^0} = (3.67 \pm 0.05)\%$, where the BF for $\Lambda \rightarrow p\pi^-$ and $\pi^0 \rightarrow \gamma\gamma$ are included. Thus, the number of the $\Lambda_c^+ \rightarrow \Lambda\pi^+\pi^0$ background events can be estimated by:

$$N_{\Lambda\pi^+\pi^0}^{\text{bkg}} = N_{\bar{\Lambda}_c^-}^{\text{tot}} \cdot \mathcal{B}(\Lambda_c^+ \rightarrow \Lambda\pi^+\pi^0) \cdot \eta_{\Lambda\pi^+\pi^0}. \quad (1)$$

Inserting the values of $N_{\bar{\Lambda}_c^-}^{\text{tot}}$, $\eta_{\Lambda\pi^+\pi^0}$ and $\mathcal{B}(\Lambda_c^+ \rightarrow \Lambda\pi^+\pi^0) = (7.01 \pm 0.42)\%$ [24] in Eq. (1), we obtain $N_{\Lambda\pi^+\pi^0}^{\text{bkg}} = 37.1 \pm 2.3$, where the uncertainties from $N_{\bar{\Lambda}_c^-}^{\text{tot}}$, $\eta_{\Lambda\pi^+\pi^0}$ and $\mathcal{B}(\Lambda_c^+ \rightarrow \Lambda\pi^+\pi^0)$ are included.

We apply a fit to the U_{miss} distribution to extract the signal yields. The $\Lambda_c^+ \rightarrow \Lambda\mu^+\nu_\mu$ signal shape is described with a function f [25], which consists of a Gaussian function to model the core of the U_{miss} distribution and two power law tails to account for the effects of ISR and FSR in the form of

$$f(U_{\text{miss}}) = \begin{cases} p_1 \left(\frac{n_1}{\alpha_1} - \alpha_1 + t\right)^{-n_1}, & t > \alpha_1, \\ e^{-t^2/2}, & -\alpha_2 < t < \alpha_1, \\ p_2 \left(\frac{n_2}{\alpha_2} - \alpha_2 - t\right)^{-n_2}, & t < -\alpha_2. \end{cases} \quad (2)$$

Here, $t \equiv (U_{\text{miss}} - U_{\text{mean}})/\sigma_{U_{\text{miss}}}$, U_{mean} and $\sigma_{U_{\text{miss}}}$ are the mean value and resolution of the Gaussian function, respectively, $p_1 \equiv (n_1/\alpha_1)^{n_1} e^{-\alpha_1^2/2}$ and $p_2 \equiv (n_2/\alpha_2)^{n_2} e^{-\alpha_2^2/2}$. The parameters α_1 , α_2 , n_1 and n_2 are fixed to the values obtained by fitting the signal MC distribution. For backgrounds, a double Gaussian function with parameters fixed according to MC simulations is used to describe the $\Lambda_c^+ \rightarrow \Lambda\pi^+\pi^0$ peaking background and a MC-derived shape

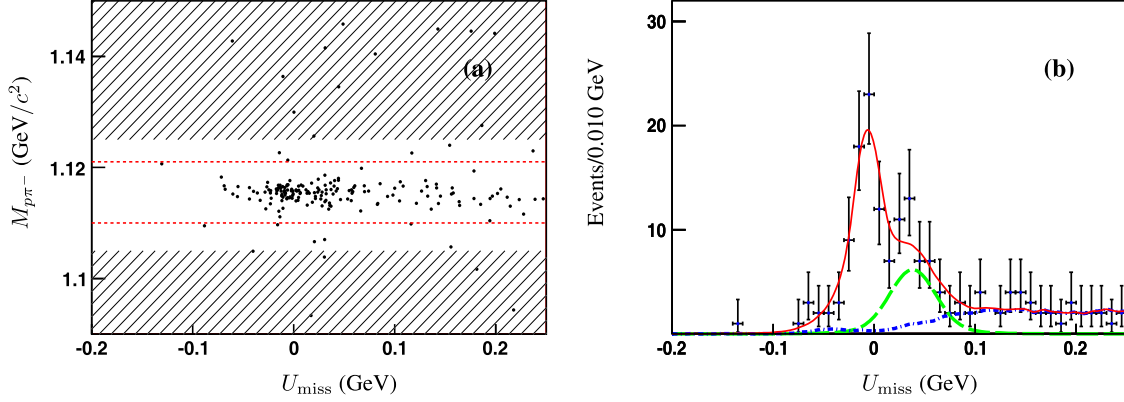


Fig. 1. (a) Distribution of $M_{p\pi^-}$ versus U_{miss} for the $\Lambda_c^+ \rightarrow \Lambda\mu^+\nu_\mu$ candidates in data. The area between the dashed lines denotes the Λ signal region and the hatched areas indicate the Λ sideband regions. (b) Fit to the U_{miss} distribution within the Λ signal region. Data are shown as dots with error bars. The long-dashed curve (green) shows the $\Lambda_c^+ \rightarrow \Lambda\pi^+\pi^0$ background contribution while the dot-dashed curve (blue) shows other contributing backgrounds. The thick line (red) shows the distribution resulting from the global fit. (For interpretation of the references to color in this figure legend, the reader is referred to the web version of this article.)

is used to describe other combinatorial backgrounds. In the fit, we fix the number of the $\Lambda_c^+ \rightarrow \Lambda\pi^+\pi^0$ background events to be estimated $N_{\Lambda\pi^+\pi^0}^{\text{bkg}}$ as described above. From the fit, we obtain the number of events of $\Lambda_c^+ \rightarrow \Lambda\mu^+\nu_\mu$ to be $N_{\Lambda\mu^+\nu_\mu}^{\text{obs}} = 78.7 \pm 10.5$, where the uncertainty is statistical only. A fit with unconstrained $N_{\Lambda\pi^+\pi^0}^{\text{bkg}}$ gives 77.1 ± 11.4 events of signal, which is in good agreement with the estimation when $N_{\Lambda\pi^+\pi^0}^{\text{bkg}}$ is fixed. Based on the data in Λ sidebands in Fig. 1(a), the background events from the non- Λ SL decays are found to be negligible.

The absolute BF for $\Lambda_c^+ \rightarrow \Lambda\mu^+\nu_\mu$ is determined by:

$$\mathcal{B}(\Lambda_c^+ \rightarrow \Lambda\mu^+\nu_\mu) = \frac{N_{\Lambda\mu^+\nu_\mu}^{\text{obs}}}{N_{\Lambda_c^+}^{\text{tot}} \cdot \varepsilon_{\Lambda\mu^+\nu_\mu} \cdot \mathcal{B}(\Lambda \rightarrow p\pi^-)}, \quad (3)$$

where $\varepsilon_{\Lambda\mu^+\nu_\mu}$ is the detection efficiency for the $\Lambda_c^+ \rightarrow \Lambda\mu^+\nu_\mu$ decay, which does not include the BF for $\Lambda \rightarrow p\pi^-$. For each ST mode i , the efficiency $\varepsilon_{\Lambda\mu^+\nu_\mu}^i$ is obtained by dividing the DT efficiency $\varepsilon_{\text{tag}, \Lambda\mu^+\nu_\mu}^i$ by the ST efficiency $\varepsilon_{\text{tag}}^i$. After weighting $\varepsilon_{\Lambda\mu^+\nu_\mu}^i$ with the ST yields in data for each ST mode i , we determine the overall average efficiency $\varepsilon_{\Lambda\mu^+\nu_\mu} = (24.5 \pm 0.2)\%$. By inserting the values of $N_{\Lambda\mu^+\nu_\mu}^{\text{obs}}$, $N_{\Lambda_c^+}^{\text{tot}}$, $\varepsilon_{\Lambda\mu^+\nu_\mu}$ and $\mathcal{B}(\Lambda \rightarrow p\pi^-)$ [22] in Eq. (3), we obtain $\mathcal{B}(\Lambda_c^+ \rightarrow \Lambda\mu^+\nu_\mu) = (3.49 \pm 0.46 \pm 0.27)\%$, where the first uncertainty is statistical, and the second uncertainty is systematic as described below.

With the DT technique, the uncertainties on the BF measurement are insensitive to those originating from the ST side. The systematic uncertainties for measuring $\mathcal{B}(\Lambda_c^+ \rightarrow \Lambda\mu^+\nu_\mu)$ mainly arise from the uncertainties related to the tracking and PID of the muon candidate, Λ reconstruction, U_{miss} fit, peaking background subtraction, $E_{\gamma\text{max}}$ and $M_{\Lambda\mu^+}$ requirements, and signal MC modelling. Throughout this paragraph, the systematic uncertainties quoted are relative uncertainties. The uncertainties of the μ^+ tracking and PID are determined to be 1.0% and 2.0%, respectively, by studying a control sample of $e^+e^- \rightarrow (\gamma)\mu^+\mu^-$ events. The uncertainty of the Λ reconstruction is determined to be 2.5% by studying a control sample of $\chi_{cJ} \rightarrow \Lambda\bar{\Lambda}\pi^+\pi^-$ decays. The uncertainty of U_{miss} fit is estimated to be 1.5% obtained by varying the fitting range and evaluating the fluctuation of the non-peaking background shape. The uncertainty due to peaking background $\Lambda_c^+ \rightarrow \Lambda\pi^+\pi^0$ subtraction is estimated to be 2.5% obtained by evaluating the variation of $N_{\Lambda\pi^+\pi^0}^{\text{bkg}}$ when the quoted BF is changed

Table 2

Summary of the sources of systematic and of the corresponding relative uncertainties for $\mathcal{B}(\Lambda_c^+ \rightarrow \Lambda\mu^+\nu_\mu)$.

Source	Uncertainty
μ^+ tracking	1.0%
μ^+ PID	2.0%
Λ reconstruction	2.5%
U_{miss} fit	1.5%
Peaking background $\Lambda_c^+ \rightarrow \Lambda\pi^+\pi^0$	2.5%
$E_{\gamma\text{max}}$ requirement	2.6%
$M_{\Lambda\mu^+}$ requirement	2.0%
MC model	5.2%
$\mathcal{B}(\Lambda \rightarrow p\pi^-)$	0.8%
$N_{\Lambda_c^+}^{\text{tot}}$	1.0%
MC statistics	0.8%
Total	7.7%

of $\pm 1\sigma$ and the shape derived from MC of the $\Lambda_c^+ \rightarrow \Lambda\pi^+\pi^0$ is smeared with a Gaussian function to accommodate the resolution difference between the data and MC simulation. The uncertainty in the $E_{\gamma\text{max}}$ requirement is estimated to be 2.6% by using a control sample of $e^+e^- \rightarrow p\bar{p}\pi^+\pi^-$ events. The uncertainty in the $M_{\Lambda\mu^+}$ requirement is estimated to be 2.0% by comparing the obtained $\mathcal{B}(\Lambda_c^+ \rightarrow \Lambda\mu^+\nu_\mu)$ under the alternative requirements of $M_{\Lambda\mu^+} < 2.07 \text{ GeV}/c^2$ or $M_{\Lambda\mu^+} < 2.17 \text{ GeV}/c^2$ with the nominal value. The uncertainty due to the MC signal modelling is estimated to be 5.2% by varying the parameterization of the form factor function according to Refs. [10,26] and by taking into account the q^2 dependence observed in data. In addition, there are systematic uncertainties from the quoted $\mathcal{B}(\Lambda \rightarrow p\pi^-)$ (0.8%), the $N_{\Lambda_c^+}^{\text{tot}}$ (1.0%) evaluated by using alternative signal shapes in the fits to the M_{BC} spectra [14], and MC statistics (0.8%). All these systematic uncertainties are summarized in Table 2, and the total systematic uncertainty is evaluated to be 7.7% by summing up all the individual contributions in quadrature.

The ratio of branching fractions $\mathcal{B}(\Lambda_c^+ \rightarrow \Lambda\mu^+\nu_\mu)/\mathcal{B}(\Lambda_c^+ \rightarrow \Lambda e^+\nu_e)$ is calculated combining $\mathcal{B}(\Lambda_c^+ \rightarrow \Lambda\mu^+\nu_\mu)$ measured in this work with $\mathcal{B}(\Lambda_c^+ \rightarrow \Lambda e^+\nu_e) = (3.63 \pm 0.38(\text{stat}) \pm 0.20(\text{syst}))\%$ from BESIII [14]. We determine $\mathcal{B}(\Lambda_c^+ \rightarrow \Lambda\mu^+\nu_\mu)/\mathcal{B}(\Lambda_c^+ \rightarrow \Lambda e^+\nu_e)$ to be $0.96 \pm 0.16 \pm 0.04$, where the first uncertainty is statistical and the second is systematic. In the ratio, common systematic uncertainties from the tracking efficiency, the Λ reconstruction, the quoted BF for $\Lambda \rightarrow p\pi^-$, the number of $\bar{\Lambda}_c^-$ tags $N_{\Lambda_c^-}^{\text{tot}}$ and the MC modelling, cancel out.

4. Summary

In summary, based on the e^+e^- collision data corresponding to an integrated luminosity of 567 pb^{-1} taken at $\sqrt{s} = 4.6 \text{ GeV}$ with the BESIII detector, we report the first direct measurement of the absolute BF for $\Lambda_c^+ \rightarrow \Lambda \mu^+ \nu_\mu$ to be $(3.49 \pm 0.46 \pm 0.27)\%$, where the first uncertainty is statistical and the second is systematic. The result is consistent with the value in PDG [22] within 2σ of uncertainty, but with improved precision. This study helps to extend our understanding on the mechanism of the Λ_c^+ SL decay. Based on this result and the previous BESIII work [14], we determine the ratio $\mathcal{B}(\Lambda_c^+ \rightarrow \Lambda \mu^+ \nu_\mu) / \mathcal{B}(\Lambda_c^+ \rightarrow \Lambda e^+ \nu_e) = 0.96 \pm 0.16 \pm 0.04$, which is compatible with unity. As the theoretical predictions on $\mathcal{B}(\Lambda_c^+ \rightarrow \Lambda e^+ \nu_e)$ vary in a large range of 1.4% to 9.2% [2–13], the measured $\mathcal{B}(\Lambda_c^+ \rightarrow \Lambda \mu^+ \nu_\mu)$ in this work and $\mathcal{B}(\Lambda_c^+ \rightarrow \Lambda e^+ \nu_e)$ in Ref. [14] provide stringent tests on these non-perturbative models, disfavoring the theoretical predictions in Refs. [2,3,5–7] at 95% confidence level.

Acknowledgements

The BESIII Collaboration thanks the staff of BEPCII and the IHEP computing center for their strong support. This work is supported in part by National Key Basic Research Program of China under Contract No. 2015CB856700; National Natural Science Foundation of China (NSFC) under Contracts Nos. 11235005, 11235011, 11305090, 11322544, 11305180, 11335008, 11425524, 11505010; the Chinese Academy of Sciences (CAS) Large-Scale Scientific Facility Program; the CAS Center for Excellence in Particle Physics (CCEPP); the Collaborative Innovation Center for Particles and Interactions (CICPI); Joint Large-Scale Scientific Facility Funds of the NSFC and CAS under Contracts Nos. U1232201, U1332201; CAS under Contracts Nos. KJXC2-YW-N29, KJXC2-YW-N45; 100 Talents Program of CAS; National 1000 Talents Program of China; INPAC and Shanghai Key Laboratory for Particle Physics and Cosmology; German Research Foundation DFG under Contracts Nos. Collaborative Research Center CRC 1044, FOR 2359; Istituto Nazionale di Fisica Nucleare, Italy; Joint Large-Scale Scientific Facility Funds of the NSFC and CAS under Contract No. U1532257; Joint Large-Scale Scientific Facility Funds of the NSFC and CAS under Contract No. U1532258; Koninklijke Nederlandse Akademie van Wetenschappen (KNAW) under Contract No. 530-4CDP03; Ministry of Development of Turkey under Contract No. DPT2006K-120470; NSFC under Contract No. 11275266; The Swedish Research Council; U.S. Department of Energy under Contracts Nos. DE-FG02-05ER41374, DE-SC-0010504, DE-SC0012069, DESC0010118; U.S. National Science Foundation; University of Groningen (RuG) and the Helmholtzzentrum fuer Schwerionenforschung GmbH (GSI), Darmstadt; WCU Program of National Research Foundation of Korea under Contract No. R32-2008-000-10155-0. This paper is also supported by the Beijing municipal government under Contracts Nos. KM201610017009, 2015000020124G064.

References

- [1] J.D. Richman, P.R. Burchat, Leptonic and semileptonic decays of charm and bottom hadrons, *Rev. Mod. Phys.* 67 (1995) 893, <http://dx.doi.org/10.1103/RevModPhys.67.893>, arXiv:hep-ph/9508250; E. Eichten, B. Hill, An effective field theory for the calculation of matrix elements involving heavy quarks, *Phys. Lett. B* 234 (1990) 511, [http://dx.doi.org/10.1016/0370-2693\(90\)92049-O](http://dx.doi.org/10.1016/0370-2693(90)92049-O); M. Neubert, Heavy quark symmetry, *Phys. Rep.* 245 (1994) 259, [http://dx.doi.org/10.1016/0370-1573\(94\)90091-4](http://dx.doi.org/10.1016/0370-1573(94)90091-4), arXiv:hep-ph/9306320.
- [2] R. Pérez-Marcial, et al., Predictions for semileptonic decays of charm baryons. II. Nonrelativistic and MIT bag quark models, *Phys. Rev. D* 40 (1989) 2955, <http://dx.doi.org/10.1103/PhysRevD.40.2955>.

- [3] M. Avila-Aoki, et al., Predictions for semileptonic decays of charm baryons. I. SU(4)-symmetry limit, *Phys. Rev. D* 40 (1989) 2944, <http://dx.doi.org/10.1103/PhysRevD.40.2944>.
- [4] F. Hussain, et al., Semi-leptonic charm baryon decays in the relativistic spectator quark model, *Z. Phys. C* 51 (1991) 607, <http://dx.doi.org/10.1007/BF01565586>.
- [5] G.V. Efimov, et al., Predictions for semileptonic decay rates of charmed baryons in the quark confinement model, *Z. Phys. C* 52 (1991) 149, <http://dx.doi.org/10.1007/BF01412338>.
- [6] Robert Singleton, Semileptonic baryon decays with a heavy quark, *Phys. Rev. D* 43 (1991) 2939, <http://dx.doi.org/10.1103/PhysRevD.43.2939>.
- [7] A. Garcia, R. Huerta, Semileptonic decays of charmed baryons, *Phys. Rev. D* 45 (1992) 3266, <http://dx.doi.org/10.1103/PhysRevD.45.3266>.
- [8] H.Y. Cheng, B. Tseng, $1/M$ corrections to baryonic form factors in the quark model, *Phys. Rev. D* 53 (1995) 1457, <http://dx.doi.org/10.1103/PhysRevD.53.1457>, arXiv:hep-ph/9502391.
- [9] H.G. Dosch, et al., QCD sum rules calculation of heavy Λ semileptonic decay, *Phys. Lett. B* 431 (1998) 173, [http://dx.doi.org/10.1016/S0370-2693\(98\)00566-8](http://dx.doi.org/10.1016/S0370-2693(98)00566-8), arXiv:hep-ph/9712350.
- [10] R.S. Marques de Carvalho, et al., Form factors and decay rates for heavy Λ semileptonic decays from QCD sum rules, *Phys. Rev. D* 60 (1999) 034009, <http://dx.doi.org/10.1103/PhysRevD.60.034009>, arXiv:hep-ph/9903326.
- [11] M. Pervin, et al., Semileptonic decays of heavy Λ baryons in a quark model, *Phys. Rev. C* 72 (2005) 035201, <http://dx.doi.org/10.1103/PhysRevC.72.035201>, arXiv:nucl-th/0503030.
- [12] Y.L. Liu, et al., Improved analysis on the semileptonic decay $\Lambda_c \rightarrow \Lambda l^+ \nu_l$ from QCD light-cone sum rules, *Phys. Rev. D* 80 (2009) 074011, <http://dx.doi.org/10.1103/PhysRevD.80.074011>, arXiv:0910.1160.
- [13] T. Gutsche, et al., Semileptonic decays $\Lambda_c^+ \rightarrow \Lambda l^+ \nu_l$ ($l = e, \mu$) in the covariant quark model and comparison with the new absolute branching fraction measurements of Belle and BESIII, *Phys. Rev. D* 93 (2016) 034008, <http://dx.doi.org/10.1103/PhysRevD.93.034008>, arXiv:1512.02168.
- [14] M. Ablikim, et al., BESIII Collaboration, Measurement of the absolute branching fraction for $\Lambda_c^+ \rightarrow \Lambda e^+ \nu_e$, *Phys. Rev. Lett.* 115 (2015) 221805, <http://dx.doi.org/10.1103/PhysRevLett.115.221805>, arXiv:1510.02610.
- [15] M. Ablikim, et al., BESIII Collaboration, Precision measurement of the integrated luminosity of the data taken by BESIII at center-of-mass energies between 3.810 GeV and 4.600 GeV, *Chin. Phys. C* 39 (2015) 093001, <http://iopscience.iop.org/1674-1137/39/9/093001>, arXiv:1503.03408.
- [16] M. Ablikim, et al., BESIII Collaboration, Design and construction of the BESIII detector, *Nucl. Instrum. Methods Phys. Res., Sect. A, Accel. Spectrom. Detect. Assoc. Equip.* 614 (2010) 345, <http://dx.doi.org/10.1016/j.nima.2009.12.050>, arXiv:0911.4960.
- [17] S. Agostinelli, et al., GEANT4 Collaboration, GEANT4 – a simulation toolkit, *Nucl. Instrum. Methods Phys. Res., Sect. A, Accel. Spectrom. Detect. Assoc. Equip.* 506 (2003) 250, [http://dx.doi.org/10.1016/S0168-9002\(03\)01368-8](http://dx.doi.org/10.1016/S0168-9002(03)01368-8).
- [18] S. Jadach, B.F.L. Ward, Z. Was, The precision Monte Carlo event generator *KK* for two-fermion final states in e^+e^- collisions, *Comput. Phys. Commun.* 130 (2000) 260, [http://dx.doi.org/10.1016/S0010-4655\(00\)00048-5](http://dx.doi.org/10.1016/S0010-4655(00)00048-5), arXiv:hep-ph/9912214; S. Jadach, B.F.L. Ward, Z. Was, Coherent exclusive exponentiation for precision Monte Carlo calculations, *Phys. Rev. D* 63 (2001) 113009, <http://dx.doi.org/10.1103/PhysRevD.63.113009>, arXiv:hep-ph/0006359.
- [19] D.J. Lange, The EvtGen particle decay simulation package, *Nucl. Instrum. Methods Phys. Res., Sect. A, Accel. Spectrom. Detect. Assoc. Equip.* 462 (2001) 152, [http://dx.doi.org/10.1016/S0168-9002\(01\)00089-4](http://dx.doi.org/10.1016/S0168-9002(01)00089-4).
- [20] E.A. Kuraev, V.S. Fadin, Radiative corrections to the cross section for single-photon annihilation of an e^+e^- pair at high energy, *Sov. J. Nucl. Phys.* 41 (1985) 466.
- [21] E. Richter-Was, QED bremsstrahlung in semileptonic B and leptonic τ decays, *Phys. Lett. B* 303 (1993) 163, [http://dx.doi.org/10.1016/0370-2693\(93\)90062-M](http://dx.doi.org/10.1016/0370-2693(93)90062-M); E. Barberio, Z. Was, PHOTOS – a universal Monte Carlo for QED radiative corrections: version 2.0, *Comput. Phys. Commun.* 79 (1994) 291, [http://dx.doi.org/10.1016/0010-4655\(94\)90074-4](http://dx.doi.org/10.1016/0010-4655(94)90074-4).
- [22] K.A. Olive, et al., Particle Data Group, *Chin. Phys. C* 38 (2014) 090001, and 2015 update, http://pdg.lbl.gov/2015/tables/contents_tables.html.
- [23] J.C. Chen, G.S. Huang, X.R. Qi, D.H. Zhang, Y.S. Zhu, Event generator for J/ψ and $\psi(2S)$ decay, *Phys. Rev. D* 62 (2000) 034003, <http://dx.doi.org/10.1103/PhysRevD.62.034003>.
- [24] M. Ablikim, et al., BESIII Collaboration, Measurements of absolute hadronic branching fractions of the Λ_c^+ baryon, *Phys. Rev. Lett.* 116 (2016) 052001, <http://dx.doi.org/10.1103/PhysRevLett.116.052001>, arXiv:1511.08380.
- [25] J.Y. Ge, et al., CLEO Collaboration, Study of $D^0 \rightarrow \pi^- e^+ \nu_e$, $D^+ \rightarrow \pi^0 e^+ \nu_e$, $D^0 \rightarrow K^- e^+ \nu_e$, and $D^0 \rightarrow \bar{K}^0 e^+ \nu_e$ in tagged decays of the $\psi(3770)$ resonance, *Phys. Rev. D* 79 (2009) 052010, <http://dx.doi.org/10.1103/PhysRevD.79.052010>, arXiv:0810.3878.
- [26] J.W. Hinson, et al., CLEO Collaboration, Improved measurement of the form factors in the decay $\Lambda_c^+ \rightarrow \Lambda e^+ \nu_e$, *Phys. Rev. Lett.* 94 (2005) 191801, <http://dx.doi.org/10.1103/PhysRevLett.94.191801>, arXiv:hep-ex/0501002.